J. Am. Chem. Soc. **2000,** *122,* 7105−7113

Conversion of Linear to Rhombic C_4 in the Gas Phase: A Joint Experimental and Theoretical Study

Stephen J. Blanksby,*,† Detlef Schröder,‡ Suresh Dua,† John H. Bowie,† and Helmut Schwarz‡

Contribution from the Department of Chemistry, The University of Adelaide, South Australia, 5005, and the Institute for Organic Chemistry, Technical University Berlin, D-10623 Berlin, Germany

Abstract: Charge reversal (CR) and neutralization reionization (NR) experiments carried out on a 4-sector mass spectrometer demonstrate that isotopically labeled, linear C_4 anion rearranges upon collisional oxidation. The cations and neutrals formed in these experiments exhibit differing degrees of isotopic scrambling in their fragmentation patterns, indicative of (at least) partial isomerization of both states. Theoretical studies, employing the CCSD(T)/aug-cc-pVDZ//B3LYP/6-31G(d) level of theory, favor conversion to the rhombic C_4 isomer on both cationic and neutral potential-energy surfaces with the rhombic structures predicted to be slightly more stable than the linear forms in each case. The combination of experiment with theory indicates that the elusive rhombic C_4 is formed as a cation and as a neutral following charge stripping of linear C_4^-.

Introduction

The volume of scientific literature pertaining to carbon clusters is testament to the intriguing nature of these species.[1,2] The participation of carbon clusters in circumstellar and interstellar chemistry,[3,4] combustion processes,[5] and material sciences[6] is well-known, but understanding their precise role in each of these systems demands detailed knowledge of the structure and reactivity of such molecules. Tetracarbon C_4 has generated particular interest and has formed the subject of intense theoretical and experimental investigations.

As early as 1977, it was proposed that neutral C_4 might have a cyclic ground state.[7] This theoretical study employing semiempirical calculations was soon followed by an ab initio investigation which revealed that the linear (**1**) $^3\Sigma_g^-$ and the rhombic (**2**) ^1A_g states are very close in energy.[8] The latter study predicted the rhombus to be the more stable by about 5 kcal mol^{-1}. More recent theoretical studies have reported the structures of **1** and **2**, their relative energies, vibrational frequencies, heats of formation, electron affinities, and ionization energies.[9−22] Most high level studies[9−11] predict that isomers **1** and **2** are virtually isoenergetic, separated at most by a few kcal mol^{-1}. Of the remaining conceivable C_4 structures only the C_3-monocyclic species (**3**) is predicted to have thermochemical stability in the same regime as **1** and **2**. This structure has been considered in early computational studies[8] and is calculated to have a singlet ground-state some 30 kcal mol^{-1} above the two almost isoenergetic isomers **1** and **2**.

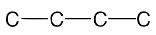
1 ($D_{\infty h}$)

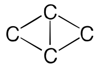
2 (D_{2h})

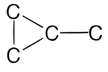
3 (C_{2v})

The cation and anion potential-energy surfaces of tetracarbon have also been investigated theoretically.[10,11,13,14,17,18] Both charged states have stable linear and cyclic forms analogous to those of the neutral. MRCI calculations by Parasuk and Almlöf predict a linear $^2\Pi_g$ ground state for the C_4^+ cation, approximately 7 kcal mol^{-1} lower in energy than the rhombic $^2B_{3u}$ isomer.[11] Recently, Giuffreda and co-workers[18] investigated the energies of cationic carbon clusters C_n^+ ($n = 4-19$) with density functional and coupled cluster theories. Their results indicate that the relative stabilities of linear and cyclic structures vary according to the method applied. However, it is clear that these species are very close in energy ($\Delta E < 4$ kcal mol^{-1}) with the rhombic structure predicted to be the most stable C_4^+ isomer at the CCSD(T) level.

---

* Correspondence to: Dr. S. J. Blanksby. Current address: Department of Chemistry and Biochemistry, University of Colorado, Boulder, Colorado 80309.

† The University of Adelaide.

‡ Technical University Berlin.

(1) Weltner, W., Jr.; Van Zee, R. J. *Chem. Rev.* **1989**, *89*, 1713 and references therein.

(2) Van Orden, A.; Saykally, R. J. *Chem. Rev.* **1998**, *98*, 2313 and references therein.

(3) Bernath, P. F.; Hinkle, K. H.; Keady, J. J. *Science* **1989**, *244*, 562.

(4) Bettens, R. P. A.; Herbst, E. *Astrophys. J.* **1997**, *478*, 585.

(5) Kroto, H. W.; McKay, K. *Nature* **1988**, *331*, 328.

(6) Levi Guyer, R.; Koshland, D. E., Jr. *Science* **1990**, *250*, 1640.

(7) (a) Slanina, Z.; Zahradnik, R. *J. Phys. Chem.* **1977**, *81*, 2252; (b) Mühlhauser, M.; Froundakis, G. E.; Hanrath, M.; Peyerimhoff, S. D. *Chem. Phys. Lett.* **2000**, *324*, 195.

(8) Whiteside, R. A.; Krishnan, R.; Defrees, D. J.; Pople, J. A.; von R. Schleyer, P. *Chem. Phys. Lett.* **1981**, *78*, 538.

(9) Martin, J. M. L.; François, J. P.; Gijbels, R. *J. Chem. Phys.* **1991**, *94*, 3753.

(10) Watts, J. D.; Gauss, J.; Stanton, J. F.; Bartlett, R. J. *J. Chem. Phys.* **1992**, *97*, 8372.

(11) Parasuk, V.; Almlöf, J. *J. Chem. Phys.* **1991**, *94*, 8172.

(12) Martin, J. M. L.; Taylor, P. R. *J. Phys. Chem.* **1996**, *100*, 6047.

(13) Watts, J. D.; Cernusak, I.; Bartlett, R. J. *Chem. Phys. Lett.* **1991**, *187*, 259.

(14) Ortiz, J. V. *J. Chem. Phys.* **1993**, *99*, 6716.

(15) Liang, C.; Schaefer, H. F., III. *Chem. Phys. Lett.* **1990**, *169*, 150.

(16) Martin, J. M. L.; Schwenke, D. W.; Lee, T. J.; Taylor, P. R. *J. Chem. Phys.* **1996**, *104*, 4657.

(17) Raghavachari, K. *Z. Phys. D* **1989**, *12*, 61.

(18) Giuffreda, M. G.; Deleuze, M. S.; François, J.-P. *J. Phys. Chem. A* **1999**, *103*, 5137.

(19) Szczepanski, J.; Vala, M.; Shen, L. N.; Whitney, P. A.; Graham, W. R. M. *J. Phys. Chem. A* **1997**, *101*, 8788.

(20) Szczepanski, J.; Ekern, S.; Vala, M. *J. Phys. Chem. A* **1997**, *101*, 1841.

(21) Bernholt, D. E.; Magers, D. H.; Bartlett, R. J. *J. Chem. Phys.* **1988**, *89*, 3612.

(22) Raghavachari, K.; Binkley, J. S. *J. Chem. Phys.* **1987**, *87*, 2191.

10.1021/ja000951c CCC: $19.00

The situation for the C_4^- anion is quite different to the neutral and cation potential-energy surfaces. Although both linear $^2\Pi_g$ and rhombic $^2B_{2g}$ anions are minima, the latter is calculated to be at least 30 kcal mol^{-1} higher in energy.[10,13] Interestingly, a recent density functional study has predicted that the monocyclic anion (**3**$^-$) is of comparable energy to the rhombic anion.[19] However, this does not significantly alter the picture of the C_4^- anion potential-energy surface where the linear structure is substantially more stable than all other isomers. Preference for formation of linear C_4^- is further evidenced by photoelectron spectra.[23−26] C_4^- anions have been generated for such experiments by laser ablation of graphite and, more recently, by pulsed discharge in an expansion of dilute acetylene/carbon dioxide mixtures. The photoelectron spectra (PES) measured in all such experiments are dominated by a pronounced peak between 3.7 and 3.9 eV, with no significant spectral features of lower energy observed. This observation is consistent with exclusive formation of the linear C_4^- anion where the corresponding neutral is predicted to have an adiabatic electron affinity (EA_a) of 3.65 eV compared with 2.24 eV for the rhombic structure.[10] The more recent PES experiments conducted with high-resolution instrumentation, measure the EA_a of linear C_4 to be 3.882 ± 0.010 eV and further identify a number of excited electronic states including two low lying singlets, $^1\Delta_g$ and $^1\Sigma_g{}^+$, which both lie less than 0.5 eV above the $^3\Sigma_g{}^-$ ground state.[25,26] These data indicate that linear C_4^- can be synthesized in the gas phase and that it is unlikely to rearrange to the much less energetically favored rhombic structure. Thus it should be possible to generate a beam of structurally pure anions which may be used to probe structures on the cationic and neutral surfaces.

McElvany has shown that C_4^- anions may be generated by laser ablation of graphite or petroleum coke.[27] These ions react slowly with very reactive species such as fluorine and cyanogen and, significantly, show a linear decay indicating the presence of a single reactive ionic species. Reactions carried out between the C_4^- anion and hydrogen sulfide, benzenethiol, and S_8 also show this behavior, which has been attributed to a linear structure.[28] Maier and co-workers have measured the laser excited emission spectrum of linear C_4^- trapped in a matrix at 5K and assigned a number of the vibrational frequencies of the linear ground state ($^2\Pi_g$) anion.[29,30] Matrix isolated carbon cluster anions have also been probed by Fourier transform infrared spectroscopy with the major absorption signals being assigned to vibrations of the linear forms.[19,20] The notable absence of rhombic C_4^- in these studies suggests either it is not generated under the experimental conditions or detection of this species is difficult.

Some evidence for the existence of rhombic C_4 as both an anion and a neutral has been provided by Coulomb explosion imaging (CEI).[31−33] In these experiments a fast beam of C_4^- anions was generated by a cesium beam sputter source, mass selected and intersected with a tuneable laser. By adjusting the laser frequency it was shown that electrons could be detached from some of the C_4^- anions at 2.1 ± 0.1 eV. This photodetachment threshold is close to 2.24 eV which is the calculated EA_a of rhombic C_4[10] and substantially lower than the EA_a of 3.88 eV measured for linear C_4.[23−26] The neutrals formed by photodetachment of the anions at 2.1 eV were then allowed to undergo high energy collisions with a thin foil, giving rapid and pronounced charge stripping and subsequent Coulomb explosion. The fragment ion distributions resulting from the explosion produced an image consistent with that predicted by modeling for C_4 with a rhombic geometry.

Numerous studies have been carried out to generate and probe the structure of neutral C_4 in both low-temperature matrices and the gas phase using spectroscopic methods.[1,2] No evidence for any structure other than linear C_4 has been forthcoming. This seems at first unusual on thermochemical grounds as calculations predict linear and rhombic C_4 to be essentially isoenergetic (see earlier). However entropic considerations predict that, in the equilibrium vaporization of graphite for example, the formation of linear C_4 is favored by a factor of about seven over formation of rhombic C_4.[34]

Cationic carbon clusters are relatively easily produced and detected in mass spectrometric experiments.[35] The C_4^+ cation has been generated by (i) electron ionization of a suitable organic carbon precursors such as diacetylene, *n*-butane,[36,37] and benzene[38] and (ii) by direct laser vaporization of graphite.[39−46] The ion−molecule chemistry of C_4^+ has been investigated by selected-ion flow tube (SIFT),[36−38] Fourier transform ion cyclotron resonance (FTICR)[39−41] and ion-beam[42−46] experiments. Regardless of the ionization method employed, these studies show linear (or near-linear) decays of the C_4^+ signals pointing to the presence of a single reactive species, which is attributed to the linear structure. Further, ion chromatography[47,48] of C_4^+ reveals a single geometric structure which is again assigned to the linear structure.[49] In summary, no definitive indications of the formation of nonlinear C_4^+ cations and only

---

(23) Yang, S. H.; Pettiette, C. L.; Conceicao, J.; Cheshnovsky, O.; Smalley, R. E. *Chem. Phys. Lett.* **1987**, *139*, 233.

(24) Yang, S. H.; Taylor, K. J.; Craycraft, M. J.; Conceicao, J.; Pettiette, C. L.; Cheshnovsky, O.; Smalley, R. E. *Chem. Phys. Lett.* **1988**, *144*, 431.

(25) Arnold, D. W.; Bradforth, S. E.; Kitsopoulos, T. N.; Neumark, D. M. *J. Chem. Phys*. **1991**, *95*, 8753.

(26) Xu, C.; Burton, G. R.; Taylor, T. R.; Neumark, D. M. *J. Chem. Phys*. **1997**, *107*, 3428.

(27) McElvany, S. W. *Int. J. Mass Spectrom. Ion Processes* **1990**, *102*, 81.

(28) Fisher, K.; Hopwood, F.; Dance, I.; Willett, G. *New J. Chem.* **1999**, *23*, 609.

(29) Freivogel, P.; Fulara, J.; Jakobi, M.; Forney, D.; Maier, J. P. *J. Chem. Phys*. **1995**, *103*, 54.

(30) Schafer, M.; Grutter, M.; Fulara, J.; Forney, D.; Freivogel, P.; Maier, J. P. *Chem. Phys. Lett*. **1996**, *260*, 406.

(31) Zajfman, D.; Feldman, H.; Heber, O.; Kella, D.; Majer, D.; Vager, Z.; Naaman, R. *Science* **1992**, *258*, 1129.

(32) Algranati, M.; Feldman, H.; Kella, D.; Malkin, E.; Miklazky, E.; Naaman, R.; Vager, Z.; Zajfman, J. *J. Chem. Phys*. **1989**, *90*, 4617.

(33) Feldman, H.; Kella, D.; Malkin, E.; Miklazky, E.; Vager, Z.; Zajfman, J.; Naaman, R. *J. Chem. Phys*. **1989**, *90*, 4617.

(34) Van Zee, R. J.; Ferrante, R. F.; Zeringue, K. J.; Weltner, W., Jr. *J. Chem. Phys*. **1988**, *88*, 3465.

(35) Parent, D. C.; Anderson, S. L. *Chem.Rev*. **1992**, *92*, 1541 and references therein.

(36) Bohme, D. K.; Wlodek, S.; Williams, L.; Forte, L.; Fox, A. *J. Chem. Phys*. **1987**, *87*, 6934.

(37) Anicich, V. G.; Huntress Jr., W. T.; McEwan, M. J. *J. Phys. Chem*. **1986**, *90*, 2446.

(38) Bohme, D. K.; Wlodek, S. *Int. J. Mass Spectrom. Ion Processes* **1990**, *102*, 133 and references therein.

(39) McElvaney, S. W.; Dunlap, B. I.; O'Keefe, A. *J. Chem. Phys*. **1987**, *86*, 715.

(40) McElvaney, S. W. *J. Chem. Phys*. **1988**, *89*, 2063.

(41) Parent, D. C.; McElvaney, S. W. *J. Am. Chem. Soc*. **1989**, *111*, 2393.

(42) Hintz, P. A.; Sowa, M. B.; Anderson, S. L. *Chem. Phys. Lett*. **1991**, *177*, 146.

(43) Sowa, M. B.; Anderson, S. L. *J. Chem. Phys*. **1992**, *97*, 8164.

(44) Sowa-Resat, M. B.; Smolanoff, J. N.; Goldman, I. B.; Anderson S. L. *J. Chem. Phys*. **1994**, *100*, 8784.

(45) Sowa-Resat, M. B.; Hintz, P. A.; Anderson, S. L. *J. Chem. Phys*. **1991**, *95*, 4719.

(46) Sowa-Resat, M. B.; Hintz, P. A.; Anderson, S. L. *J. Phys. Chem*. **1995**, *99*, 10736.

(47) Bowers, M. T.; Kemper, P. R.; von Helden, G.; van Koppen, P. A. M. *Science* **1993**, *260*, 1446 and references therein.

(48) Jarrold, M. F. *J. Phys. Chem*. **1995**, *99*, 11 and references therein.

(49) von Helden, G.; Hsu, M.; Gotts, N.; Bowers, M. T. *J. Phys. Chem*. **1993**, *97*, 8182.

limited evidence for the existence of rhombic structures for neutral and anionic tetracarbon have been reported.

In this study, we examine linear C_4^- anions in conjunction with ^{13}C labeling experiments. High-energy collisions of the mass selected anions are used to produce neutral and cationic C_4. The isotope distributions observed in charge reversal (CR) and neutralization reionization (NR) experiments suggest that tetracarbon is rearranging as a cation and as a neutral. Theoretical calculations indicate that the energetically preferred pathway to $^{12}C/^{13}C$ equilibration involves the conversion of linear to rhombic structures for neutral and cationic tetracarbon.

Experimental Section

A. Mass Spectrometric Methods. For a detailed description of the experiment and the instrument used see Schalley et al.[50] In brief, the experiments were performed using a four-sector modified HF-ZAB/AMD 604 mass spectrometer with BEBE configuration, where B and E represent magnetic and electric sectors, respectively. The C_4^- anion was generated by chemical ionization (CI) in the negative ion mode, with typical source conditions as follows: source temperature 200 °C, repeller voltage −0.5 V, ion extraction voltage 8 kV, mass resolution $m/\Delta m \geq 1500$. Bis(trimethylsilyl)butadiyne was placed in a small glass capillary tube which was then drawn out in a flame to create a very fine aperture, allowing for a slow steady release of sample vapor upon heating. The capillary was inserted into the CI source via the direct probe; the probe tip was heated to 60−80 °C to generate a background pressure of $\sim10^{-5}$ Torr inside the source housing. The C_4^- anion was formed following double desilylation, utilizing SF_6 as a CI reagent gas at a pressure of $\sim10^{-4}$ Torr inside the source housing. Double desilylation has been shown to be a successful method for the generation of radical anions and is similar to the method first introduced by Squires and co-workers using F_2/NF_3 mixtures.[51]

Collisional induced dissociation (CID) of B(1)/E(1)-mass selected ions was effected in collision cells positioned between E(1) and B(2). Helium was used as a target gas. The pressure of the collision gas in the cell was maintained such that 80% of the parent ion beam was transmitted through the cell. This corresponds to an average of 1.1−1.2 collisions per ion.[52] Product ions resulting from CID were recorded by scanning the second magnetic sector B(2).

Neutralization−reionization[53,54] ($^-NR^+$) experiments were performed for B(1)/E(1)-mass selected C_4^- utilizing the dual collision cells located between sectors E(1) and B(2). Neutralization of the anions was achieved by collisional electron detachment using O_2 at 80% transmittance as collision gas, while reionization to cations was achieved by collision of the neutrals with O_2, again at 80% transmittance. Any ions remaining after the first collision event were deflected from the primary neutral beam using an electrode maintained at a high voltage (1.5 kV) positioned before the second collision cell. To detect a reionization signal due to the parent, the neutral species must be stable for approximately one microsecond. Charge reversal ($^-CR^+$) spectra[55−57] were recorded under both, $^-NR^+$ conditions (O_2/O_2, 80%T/80%T; deflector electrode grounded) and single collision conditions (O_2, 80%T). No significant differences were observed in $^-CR^+$ spectra measured by these procedures. Collection of $^-CR^+$ and $^-NR^+$ spectra under the same experimental conditions allows for a direct comparison to be made from which it is possible to infer the behavior of the intermediate neutral on the NR time scale (10^{-6} s).[58−60] $^-NR^+$, $^-CR^+$, and CID spectra were averaged over 10−20 acquisitions in order to obtain sufficient signal-to-noise (S/N) ratios. $^-NR^-$ experiments gave peaks of significantly lower intensity (compared with $^-NR^+$ experiments). The $^-NR^-$ experiments were conducted as follows: mass selection of the parent anion with B(1), neutralization by collision with O_2 at 60% transmittance, reionization to anions by collision of the neutrals with Xe at 70% transmittance, and the spectra measured by scanning E(1).

B. Synthesis of Labeled Precursors. 1,4-Bis(trimethylsilyl)-1,3-butadiyne. $(CH_3)_3Si{-}C{\equiv}C{-}C{\equiv}C{-}Si(CH_3)_3$ was obtained as a commercial sample (*ABCR*) and used without further purification. MS (EI, 70 eV), *m/z* 196(2), 195(5), 194(22), 181(6), 180(12), 179(100), 121(7), 107(4), 97(11), 83(7), 82(16), 73(16).

[1,4-$^{13}C_2$]-But-2-yne-1,4-diol. According to the procedure proposed by Wolf and Spenser,[61] 1,1,2-trichloroethene (1.11 g, 8.4 mmol) in anhydrous diethyl ether (20 mL) was added dropwise under anhydrous nitrogen to a stirred solution of *n*-butyllithium (16.3 mL, 1.6 M in hexane, 26 mmol) in diethyl ether/tetrahydrofuran [(1:1) 100 mL) at −78 °C, over 10 min.[62] The solution was then stirred for 4 h at 25 °C before [^{13}C]-paraformaldehyde (0.31 g, Cambridge Isotopes, 99 atom % ^{13}C, 10.0 mmol) was added and the mixture stirred for 12 h. Further [^{13}C]-paraformaldehyde (0.24 g, 7.7 mmol) was added followed by stirring for 1 h after which time the mixture was refluxed for 1 h, water (0.6 mL) was added to the reaction and refluxing continued for 10 min. Ion-exchange resin (6 g, Amberlite CG 50-100) was added to the cooled solution (25 °C) and the mixture stirred for 30 min before being filtered, the resin washed with tetrahydrofuran (30 cm^3), and the solvent removed in vacuo giving an oily orange residue (1.3 g) which was used without further purification.

1,4-Bis(toluene-4-sulfonyloxy)-[1,4-$^{13}C_2$]-but-2-yne. All recovered crude [1,4-$^{13}C_2$]-but-2-yne-1,4-diol was dissolved in anhydrous tetrahydrofuran (35 mL), tosyl chloride (3.22 g, 17 mmol) was added and the mixture cooled to −15 °C before potassium hydroxide (0.95 g, 17 mmol) in water (3 mL), cooled to 0 °C, is added dropwise over 30 min with stirring. The reaction was maintained at −15 °C for 1.5 h before further potassium hydroxide (0.32 g, 6 mmol), in water (2 mL), was added dropwise over 30 min followed by stirring at −15 °C for a further 1h. The mixture was poured onto ice (35 g), warmed to room temperature and extracted with dichloromethane (3 × 30 mL). The combined organic extracts were dried ($MgSO_4$) and the solvent removed in vacuo to give an oily orange residue which was purified by chromatography over silica, eluting with dichloromethane/pentane (1:1), yielding a colorless solid (1.50 g, 3.8 mmol, 43% yield based on $^{13}CH_2O$).

1,4-Bis(trimethylsilyl)-1,3-[1,4-$^{13}C_2$]-butadiyne. 1,4-Bis(toluene-4-sulfonyloxy)-[1,4-$^{13}C_2$]-but-2-yne (1.5 g, 3.8 mmol) in anhydrous tetrahydrofuran (50 mL) was cooled to −78 °C under dry nitrogen and *n*-butyllithium (10 mL, 1.6 M in hexane, 16 mmol) was added dropwise over 30 min. The mixture was stirred for 1 h at −78 °C, warmed to −40 °C for 30 min, cooled to −78 °C and trimethylsilyl chloride (2.2 g, 20 mmol) in tetrahydrofuran (50 mL) was added over 30 min. The mixture was slowly warmed to room temperature and stirred for 12 h before addition of aqueous ammonium chloride (saturated, 20 mL). The mixture was extracted with diethyl ether (3 × 30 mL), the combined ethereal extracts were washed with water (20 mL) and aqueous sodium chloride (20 mL), dried ($MgSO_4$), and the solvent removed in vacuo. The crude product was then purified by chromatography over silica, eluting with pentane, yielding a light brown crystalline solid (0.26 g, 1.3 mmol, overall 15% yield based on $^{13}CH_2O$). MS (EI, 70 eV), *m/z* 198(2), 197(4), 196(20), 183(7), 182(14), 181(100), 123(6), 109(3), 98(7), 84(5), 83(12), 73(14).

C. Theoretical Methods. Geometry optimizations were carried out with the Becke 3LYP method[63,64] using a modest 6-31G(d) basis within

---

[50] Schalley, C. A.; Hornung, G.; Schröder, D.; Schwarz, H. *Chem. Soc. Rev.* **1998**, *27*, 91.

[51] Wenthold, P. G.; Hu, J.; Squires, R. R. *J. Am. Chem. Soc.* **1994**, *116*, 6961.

[52] Holmes, J. L. *Org. Mass Spectrom.* **1985**, *20*, 169.

[53] Goldberg, N.; Schwarz, H. *Acc. Chem. Res.* **1994**, *27*, 347.

[54] Zagorevskii, D. V.; Holmes, J. H. *Mass Spectrom. Rev.* **1994**, *13*, 133.

[55] Bowie, J. H.; Blumenthal, T. *J. Am. Chem. Soc.* **1975**, *97*, 2959.

[56] Szulejko, J. E.; Bowie, J. H.; Howe, I.; Beynon, J. H. *Int. J. Mass Spectrom. Ion Phys.* **1980**, *13*, 76.

[57] Bursey, M. M. *Mass Spectrom. Rev.* **1990**, *9*, 555.

[58] Schalley, C. A.; Blanksby, S. J.; Harvey, J. N.; Schröder, D.; Zummack, W.; Bowie, J. H.; Schwarz, H. *Eur. J. Org. Chem.* **1998**, 987.

[59] Schalley, C. A.; Hornung, G.; Schröder, D.; Schwarz, H. *Int. J. Mass Spectrom. Ion Processes* **1998**, *172/173*, 181.

[60] Hornung, G.; Schalley, C. A.; Dieterle, M.; Schröder, D.; Schwarz, H. *Chem Eur. J.* **1997**, *3*, 1866.

[61] Wolf, E.; Spenser, I. D. *J. Org. Chem.* **1995**, *60*, 6937.

[62] Uhlig, W. *J. Organometallic Chem.* **1997**, *545−546*, 281.

[63] Becke, A. D. *J. Phys. Chem.* **1993**, *98*, 5648.

Scheme 1

$$\mathrm{(CH_3)_3Si{-}C{\equiv}C{-}C{\equiv}C{-}Si(CH_3)_3 \ + \ SF_6^- \ \rightarrow \ (CH_3)_3Si{-}C{\equiv}C{-}C{\equiv}C^- \ + \ SF_5 \ + \ (CH_3)_3SiF}$$

$$\mathrm{(CH_3)_3Si{-}C{\equiv}C{-}C{\equiv}C^- \ + \ SF_5 \ \rightarrow \ C{\equiv}C{-}C{\equiv}C^- \ + \ SF_4 \ + \ (CH_3)_3SiF}$$

Scheme 2

$$\text{(a)} \quad \mathrm{(CH_3)_3Si{-}C{\equiv}C{-}C{\equiv}C{-}Si(CH_3)_3 \ + \ SF_6^- \ \rightarrow \ C{\equiv}C{-}C{\equiv}C^- \ + \ SF_4 \ + \ 2\,(CH_3)_3SiF}$$

$$\text{(b)} \quad \mathrm{(CH_3)_3Si{-}{}^{13}C{\equiv}C{-}C{\equiv}{}^{13}C{-}Si(CH_3)_3 \ + \ SF_6^- \ \rightarrow \ {}^{13}C{\equiv}C{-}C{\equiv}{}^{13}C^- \ + \ SF_4 \ + \ 2\,(CH_3)_3SiF}$$

the GAUSSIAN 94 suite of programs.[65] Stationary points were characterized as either minima (no imaginary frequencies) or transition structures (one imaginary frequency) by calculation of the frequencies using analytical gradient procedures. The minima connected by a given transition structure were confirmed by intrinsic reaction coordinate (IRC) calculations. The calculated frequencies were also used to determine zero-point vibrational energies which were then scaled[66] by 0.9804 and used as a zero-point correction for the electronic energies calculated at this and higher levels of theory. B3LYP/6-31G(d) has previously been used for geometry optimizations of anionic carbon clusters and has demonstrated good correlation with structures calculated using pure ab initio approaches.[20] Our study also points to generally good agreement between the geometries predicted using this economic hybrid-density functional approach and the more costly methods employed by other groups (see Tables 2−5 for comparison). Some problems have been highlighted in the literature regarding the use of the B3LYP method for the accurate prediction of molecular energies for carbon clusters.[67] Consequently, more accurate energies for the B3LYP geometries were determined using the CCSD(T) method[68−73] together with the Dunning aug-cc-pVDZ basis set.[74,75] The CCSD(T)/aug-cc-pVDZ//B3LYP/6-31G(d) approach predicts the adiabatic electron affinity of linear C_4 to be 3.65 eV which is in reasonable agreement with the experimentally measured value of 3.88 eV.[25,26] All calculations were carried out on Power Challenge Supercomputers at either the South Australian Supercomputing Centre (Adelaide) or the Australian National University Supercomputing Facility (Canberra).

Results and Discussion

A. Formation of Linear C_4^-. In these experiments, the C_4^- anion was formed by introducing bis(trimethylsilyl)butadiyne $\mathrm{(CH_3)_3Si{-}C{\equiv}C{-}C{\equiv}C{-}Si(CH_3)_3}$ into the source of the mass spectrometer in the presence of sulfur hexafluoride SF_6 which acts as the ionizing reagent. The exact mechanism for this process is not known; however, it seems likely to follow a similar pathway to that suggested by Squires and co-workers[51] for double desilylation reactions initiated by fluorine and/or NF_3. A plausible reaction pathway is given in Scheme 1. The C_4^- anion formed in this reaction is expected to be linear (**1**$^-$) in accordance with the connectivity of the carbon chain in the precursor molecule. Rearrangement of the initially formed linear structure also seems unlikely given the high-energy requirements of such a process (endothermic by more than 25 kcal mol^{-1} with barriers of more than 30 kcal mol^{-1}, see Figure 1 and subsequent theoretical discussion). Negative ion chemical ionization is generally regarded as a soft ionization technique, and it is therefore unlikely that the energy required for structural rearrangement would be imparted during this process. This is confirmed by the enthalpy of the reaction according to Scheme 2a which is approximated from thermochemical data available in the literature[77] to be endothermic by 8 kcal mol^{-1}. Accordingly, the initially formed linear C_4^- anion is energetically cold and rearrangement seems improbable.

This method of gas-phase synthesis of C_4^- lends itself to the incorporation of isotopic labels through the use of ^{13}C-labeled bis(trimethylsilyl)butadiyne as a precursor molecule (Scheme 2b). The fragmentation of the labeled anion should give further insight into the connectivities of this species. The CID spectrum of labeled C_4^- shows only two fragment anions at m/z 37 and 25 corresponding to losses of ^{13}C and ^{12}C^{13}C respectively (Table 1). These results are consistent with the simple cleavages of the linear C_4^- anion, **1**$^-$, where the ^{13}C atoms occupy terminal positions. Other anion structures such as **2**$^-$ and **3**$^-$ would be expected to show some losses of ^{12}C, $^{12}C_2$, and $^{13}C_2$ under CID conditions. The absence of such fragments confirms that C_4^- formed as outlined in Scheme 2 has not undergone equilibration of the carbon atoms and is hence assumed to be the linear isomer.

B. Stability of C_4^-. The Becke 3LYP method was employed with the modest 6-31G(d) basis to calculate molecular geometries across the anion, neutral and cation potential-energy surfaces of C_4. These computations show reasonable to good agreement with previous theoretical studies, some of which have

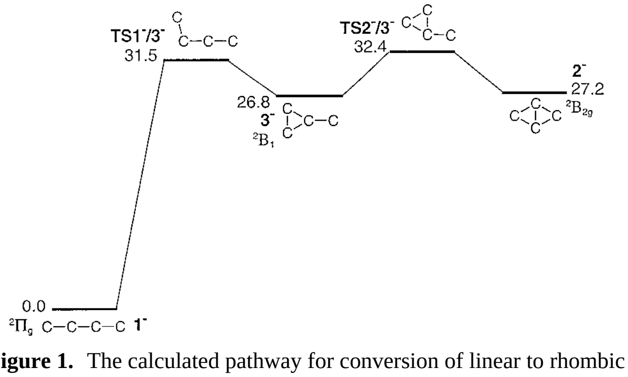

Figure 1. The calculated pathway for conversion of linear to rhombic C_4 on the anion potential energy surface. The energies are given in kcal mol^{-1} and were calculated at the CCSD(T)/aug-cc-pVDZ//B3LYP/6-31G(d) level of theory. The geometric details for these minima and transition structures are given in Table 2.

---

[64] Stevens, P. J.; Devlin, F. J.; Chablowski, C. F.; Frisch, M. J. *J. Phys. Chem.* **1994**, *98*, 11623.

[65] Frisch, M. J.; Trucks, G. W.; Schlegel, H. B.; Gill, P. M. W.; Johnson, B. G.; Robb, M. A.; Cheeseman, J. R.; Keith, T.; Peterson, G. A.; Montgomery, J. A.; Raghavachari, K.; Al- Laham, M. A.; Zakrzewski, V. G.; Ortiz, J. V.; Foresman, J. B.; Peng, C. Y.; Ayala, P. Y.; Chen, W.; Wong, M. W.; Andres, J. L.; Replogle, E. S.; Gomperts, R.; Martin, R. L.; Fox, D. J.; Binkley, J. S.; Defrees, D. J.; Baker, J.; Stewart, J. P.; Head-Gordon, M.; Gonzales, C.; Pople, J. A. *Gaussian 94*, revision B3; Gaussian Inc.: Pittsburgh, PA, 1995.

[66] Wong, M. W. *Chem. Phys. Lett.* **1996**, *256*, 391.

[67] Plattner, D. A.; Houk, K. N. *J. Am. Chem. Soc.* **1995**, *117*, 4405.

[68] Cizek, J. *Adv. Chem. Phys.* **1969**, *14*, 35.

[69] Pople, J. A.; Krishnan, R.; Schlegel, H. B.; Binkley, J. S. *Int. J. Quantum Chem.* **1978**, *14*, 545.

[70] Hampel, C.; Peterson, K.; Werner, H.-J. *Chem. Phys. Lett.* **1992**, *190*, 1.

[71] Watts, J. D.; Gauss, J.; Bartlett, R. J. *J. Chem. Phys.* **1993**, *98*, 8718.

[72] Knowles, P. J.; Hampel, C.; Werner, H.-J. *J. Chem. Phys.* **1993**, *99*, 5219.

[73] Deegan, M. J. O.; Knowles, P. J. *Chem. Phys. Lett.* **1994**, *227*, 321.

[74] Dunning, T. H. *J. Chem. Phys.* **1989**, *90*, 1007.

[75] Woon, D. E.; Dunning, T. H. *J. Chem. Phys.* **1993**, *98*, 1358.

[76] http://webbook.nist.gov and references therein.

[77] This estimation is based on the following heats of formation: $\Delta H_f°[\mathrm{(CH_3)_3SiC{\equiv}CC{\equiv}CSi(CH_3)_3}] = 8.9$ kcal mol^{-1},[78] $\Delta H_f°[\mathrm{SiF_6^-}] = -316$ kcal mol^{-1},[79] $\Delta H_f°[\mathrm{C_4^-}] = 155$ kcal mol^{-1},[76] $\Delta H_f°[\mathrm{FSi(CH_3)_3}] = -135.9$ kcal mol^{-1},[79] and $\Delta H_f°[\mathrm{SiF_4}] = -182.4$ kcal mol^{-1}.[76]

Table 1. CID and $^-$NR$^-$ Spectra of the ^{13}C Labeled C_4^- Anion. $^-$CR$^+$, $^-$NR$^+$ and $^-$NR$^-$ Spectra of the Unlabeled C_4^- Anion

precursor ion	spectrum type (collision conditions)	fragmentations mass/charge ratio (relative intensity)
^{13}C−C−C-^{13}C$^-$	CID (He, 90%T)	37 (100), 25 (17)
^{13}C−C−C-^{13}C$^-$	$^-$NR$^-$ (O_2, 60%T; Xe, 70%T)[a]	50(100), 38(4), 37(4), 26(<1),[b] 25(3), 24(<1)[b]
C−C−C−C$^-$	$^-$CR$^+$ (O_2, 80%T; O_2, 80%T)	48 (100), 36 (32), 24 (10), 12 (7)
C−C−C−C$^-$	$^-$NR$^+$ (O_2, 80%T; O_2, 80%T)	48 (100), 36 (44), 24 (11), 12 (9)
C−C−C−C$^-$	$^-$NR$^-$ (O_2, 60%T; Xe, 70%T)	48 (100), 36 (4), 24 (2)

[a] This spectrum is very weak and was determined using the maximum sensitivity of the instrument. Three single scans were performed—the listed abundances of the fragment ions are correct to ±20%. [b] These peaks are superimposed on significant baseline noise in this spectrum and are just observable. The ratio of $^{12}C_2^-$:$^{12}C^{13}C^-$:$^{13}C_2^-$ expected for randomization of carbon label is 1:4:1.

Table 2. Minima and Transition Structures on the C_4^- Anion Surface Calculated at the B3LYP/6-31G(d) Level of Theory, with Single Point Energies (Including Zero-Point Energy Correction) Computed at CCSD(T)/aug-cc-pVDZ

	$C_1-C_2-C_3-C_4$ **1$^-$**	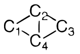 **2$^-$**	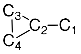 **3$^-$**	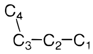 **TS1$^-$/3$^-$**	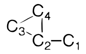 **TS2$^-$/3$^-$**
State	$^2\Pi_g$ ($^2\Pi_g$)[a]	$^2B_{2g}$ ($^2B_{2g}$)[a]	$^2B_1$	-	$^2A''$
Symmetry	$D_{\infty h}$ ($D_{\infty h}$)[a]	C_{2h} (C_{2h})[a]	C_{2v}	C_1	C_S
Energy (Hartrees)	-151.80442	-151.76109	-151.76171	-151.75426	-151.75280
Rel. Energy (kcal mol^{-1})	0.0	27.2 (30.0)[a]	26.8	31.5	32.4
Bond Lengths (Å)					
C_1-C_2	1.281 (1.266)[a]	1.460 (1.441)[a]	1.306	1.291	1.328
C_2-C_3	1.341 (1.328)[a]	-	1.505	1.416	1.440
C_3-C_4		-	1.347	1.314	1.4043
C_2-C_4		1.459 (1.450)[a]			1.544
Bond Angles (°)					
C_1-C_2-C_3		120.1 (119.6)[a]	153.4	178.6	142.6
C_2-C_3-C_4		59.9 (60.4)[a]	63.4	88.7	65.8
Dihedral Angles (°)				-137.6	

[a] Calculated at the UHF-CCSD/PVTZ level.[10]

been carried out using high level ab initio approaches (Tables 2−5). The energies of these B3LYP/6-31G(d) structures were calculated using the more rigorous CCSD(T)/aug-cc-pVDZ approach and generally agree well with available theoretical and even experimental data.

Three minima were located on the anion surface, with linear **1**$^-$ found to be more stable than rhombic **2**$^-$ and the monocyclic structure **3**$^-$ by 27.2 and 26.8 kcal mol^{-1} respectively. Isomerization of **1**$^-$ to **3**$^-$ requires 31.5 kcal mol^{-1} to overcome the barrier through transition structure **TS1**$^-$**/3**$^-$ (Figure 1). Rhombic anion (**2**$^-$) can be formed from **3**$^-$ via transition structure **TS2**$^-$**/3**$^-$ which is located 32.4 kcal mol^{-1} above **1**$^-$. Given that the two transition structures are so close in energy (separated by less than 1 kcal mol^{-1}) it is likely that rearrangement of **1**$^-$ to **3**$^-$ would also result in formation of **2**$^-$. These calculations suggest that rearrangement of the C_4^- anion is less energetically demanding than either; (i) electron detachment which requires 84, 54, and 80 kcal mol^{-1} for **1**$^-$, **2**$^-$, and **3**$^-$, respectively (see Tables 2, 4, and 5) or (ii) possible dissociations which have endothermicities estimated to be 166 and 170 kcal mol^{-1} for the fragmentations, $C_4^- \rightarrow C_3^- + C$ and $C_4^- \rightarrow C_2^- + C_2$ respectively (based on linear C_4^- and data from ref 76). This is an interesting finding given that the CID spectrum of the ^{13}C labeled anion shows clearly that fragmentation of the anion occurs without skeletal rearrangement.

C. Formation of C_4^+. The structure and stability of the C_4^+ cation may be investigated using the corresponding anion as a precursor via the charge reversal ($^-$CR$^+$) experiment. Here the incident anion undergoes two electron oxidation by collision with oxygen gas, the nascent cation and any cationic fragments are detected and form the charge reversal spectrum. The $^-$CR$^+$ spectrum of unlabeled C_4^- is given in Table 1 and shows a clear recovery signal, that is a peak at *m/z* 48 corresponding to C_4^+, and fragment ions C_3^+, C_2^+, and C^+. As for the anion, incorporation of the isotopic label should give some insight into the structure(s) of the cations formed in this process. If the linear structure of the anion is retained and the linear cation (**1**$^+$) is formed and it is this species which fragments, exclusive losses of ^{13}C, ^{13}C^{12}C (cf. the negative ion CID spectrum discussed above), and ^{13}C^{12}C$_2$ should be observed in the $^-$CR$^+$ spectrum. The $^-$CR$^+$ spectrum of isotopically labeled C_4^- is shown in Figure 2a. While fragmentations corresponding to all possible combinations of ^{12}C and ^{13}C are observed, the losses are not statistical and therefore do not correspond to a complete scrambling of the label. For example, the peaks *m/z* 37 and 38 correspond to losses of ^{13}C and ^{12}C, respectively. The ratio of the abundances of these peaks is approximately 5:3 (Figure 2a), rather than 1:1 as anticipated for complete ^{12}C/^{13}C equilibration. Similarly, the abundances of peaks at *m/z* 24, 25, and 26, which correspond to the $^{12}C_2^+$, $^{12}C^{13}C^+$, and $^{13}C_2^+$ fragments, respectively, do not appear in the statistical 1:4:1 ratio, but 1.3:8:1.0.

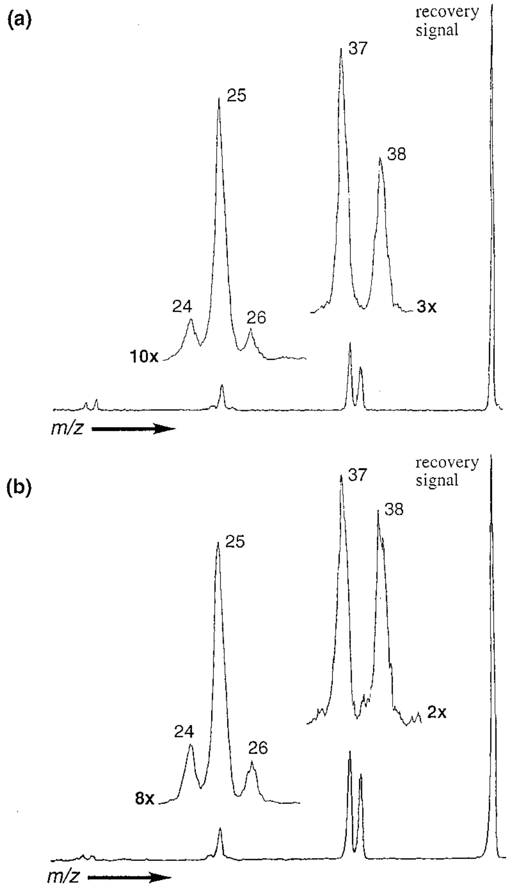

Figure 2. Charge inversion spectra of the ^{13}CCC^{13}C$^-$ anion, (a) $^-$CR$^+$ spectrum (O_2/O_2, 80%T/80%T; deflector electrode grounded), (b) $^-$NR$^+$ spectrum (O_2/O_2, 80%T/80%T; deflector electrode active). The inset expansions, shown for each spectrum, were measured independently and were averaged over 20−30 acquistions.

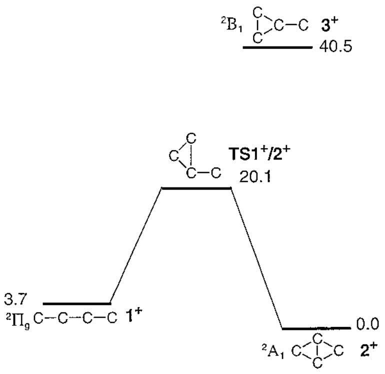

Figure 3. The calculated pathway for conversion of linear to rhombic C_4 on the cation potential energy surface. The energies are given in kcal mol^{-1} and were calculated at the CCSD(T)/aug-cc-pVDZ//B3LYP/6-31G(d) level of theory. The geometric details for these minima and transition structures are given in Table 3.

Table 3. Minima and Transition Structures on the C_4^+ Cation Surface Calculated at the B3LYP/6-31G(d) Level of Theory, with Single Point Energies (Including Zero-Point Energy Correction) Computed at CCSD(T)/aug-cc-pVDZ

	$C_1{-}C_2{-}C_3{-}C_4$ **1^+**	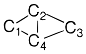 **2^+**	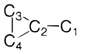 **3^+**	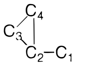 **$TS1^+/2^+$**
State	$^2\Pi_g$ ($^2\Pi_g$)^a	$^2A_1$	$^2B_1$	$^2A'$
Symmetry	$D_{\infty h}$ ($D_{\infty h}$)^a	C_{2v} ^{b}	C_{2v}	C_S
Energy (Hartrees)	-151.27947	-151.28538	-151.22090	-151.25332
Rel. Energy (kcal mol^{-1})	3.7	0.0	40.5	20.1
Bond Lengths (Å)				
C_1-C_2	1.372 (1.351)^a	1.395	1.304	1.382
C_2-C_3	1.264 (1.260)	1.483	1.468	1.314
C_3-C_4			1.355	1.406
C_2-C_4		1.645		1.739
Bond Angles (°)				
C_1-C_2-C_3		110.2	152.5	152.2
C_2-C_3-C_4		67.4	62.5	79.4

[a] Calculated at the MRCI/**S**[421]//CASSCF/**G**[431] level.[11] [b] A C_{2h} stationary point closely approximating the literature structure[11] (given in brackets) was also located in this study: $C_1{-}C_2 = 1.437$ (1.427) Å, $C_1{-}C_2{-}C_3 = 108.8$ (105.2)°. It possesses a negative frequency and is isoenergetic to the C_{2v} minimum described here. The two structures (C_{2v} and C_{2h}) may be considered experimentally equivalent, and the structure of highest symmetry is used in discussions and schematics throughout the text.

While the predominant $^{12}C^{13}C^+$ fragment is again in keeping with anion formation according to Scheme 2b, the observed scrambling indicates a rearrangement of the carbons within the C_4 skeleton. As C_4^- does not rearrange (see above), the partial scrambling observed in the $^-CR^+$ spectrum points to rearrangement of the cation prior to fragmentation. Possible rearrangement pathways and intermediates have been considered theoretically and the results are outlined below.

D. Rearrangement of C_4^+. Three minima were located on the C_4^+ cation surface (Table 3). The linear (**1^+**) and rhombic (**2^+**) structures were found to be very close energetically with the latter more stable by just 3.7 kcal mol^{-1}. Transition structure (**$TS1^+/2^+$**) connecting these two species is located 20.1 kcal mol^{-1} above the global minimum. This suggests that if the linear cation is formed with only 16.4 kcal mol^{-1} excess internal energy, an equilibrium between it and the rhombic structure may be established (Figure 3). The minimum internal energy imparted to the charge reversed ion during a single, two-electron oxidation step depends on the Franck–Condon overlap between anion and cation structures. If we consider the structures of **1^-** and **1^+** it is apparent that, while both are $D_{\infty h}$ geometries, their bond lengths differ substantially (Tables 2 and 3). A single point calculation of the optimized linear anion geometry on the cationic doublet surface at the CCSD(T)/aug-cc-pVDZ//B3LYP/6-31G(d) level of theory gives an energy 16.2 kcal mol^{-1} above that of the optimized cation structure. Thus, vertical two-electron oxidation of the ground-state anion in a $^-CR^+$ experiment deposits some 16.2 kcal mol^{-1} excess energy in the cation formed. This amount of energy suggests that a proportion of the cations formed in the experiment will rearrange to the more stable rhombic structure. The calculated barrier for rearrangement via **$TS1^+/2^+$** falls well below; (i) the relative energy of structure **3^+** which is nearly 41 kcal mol^{-1} above **2^+** and (ii) the estimated energy of the cation dissociation channels $C_4^+ \rightarrow C_3^+ + C$ and $C_4^+ \rightarrow C_2^+ + C_2$ have endothermicities of 134 and 130 kcal mol^{-1} respectively (from available data[10,76] and based on a linear C_4 structure).

Scheme 3

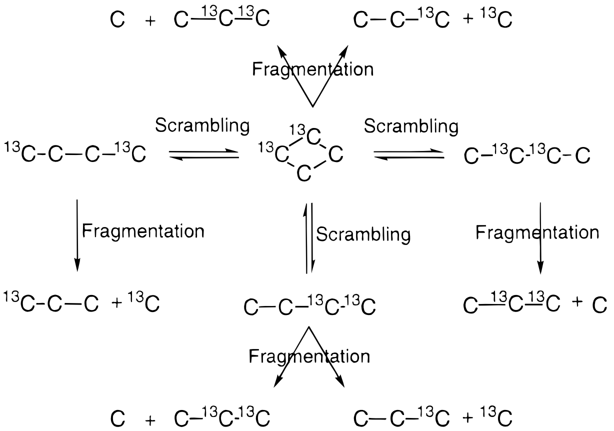

Having demonstrated that the linear C_4^+ cations formed in the $^-CR^+$ experiment have the potential to rearrange to the more stable rhombic structure, it remains to consider how this would affect the distribution of the isotopic label in the corresponding ^{13}C experiment. Rearrangement of the labeled linear cation (as described in Figure 3) is shown in Scheme 3 along with the possible, $C_4^+ \rightarrow C_3^+ + C$, fragmentations for each structure (charges are not shown in Scheme 3 for simplicity). Simple cleavages of the terminal carbons are assumed for linear structures: labeled rhombic C_4 should lose both ^{12}C and ^{13}C statistically. Scheme 3 demonstrates that if an equilibrium is established between rhombic and linear cations, subsequent fragmentation would give equivalent losses of ^{12}C and ^{13}C. A similar analysis may be applied to distribution of the label in the fragmentation $C_4^+ \rightarrow C_2^+ + C_2$.

Scrambling of the ^{13}C labels during the CR experiment may therefore be attributed to a certain population of the linear cations (**1^+**) formed with sufficient energy to rearrange to the rhombic C_4 cation (**2^+**) prior to fragmentation. The intermediacy of other isomers, such as **3^+**, cannot be completely discounted but these are likely to play a lesser role based on energy considerations. It is also probable that some linear C_4^- anions will dissociate directly upon charge reversal with no prior rearrangement giving fragments consistent with the original isotopic distribution. Therefore, in the $^-CR^+$ experiment there exists competition between (i) those cations which dissociate directly and hence maintain the original isotopic distribution and, (ii) those which rearrange (Figure 3) prior to dissociation generating scrambling of the label (Scheme 3). Such competition would result in the nonstatistical distribution of isotopic fragments observed in the $^-CR^+$ spectrum; both pathways are illustrated in Figure 4. It should also be noted that some cations

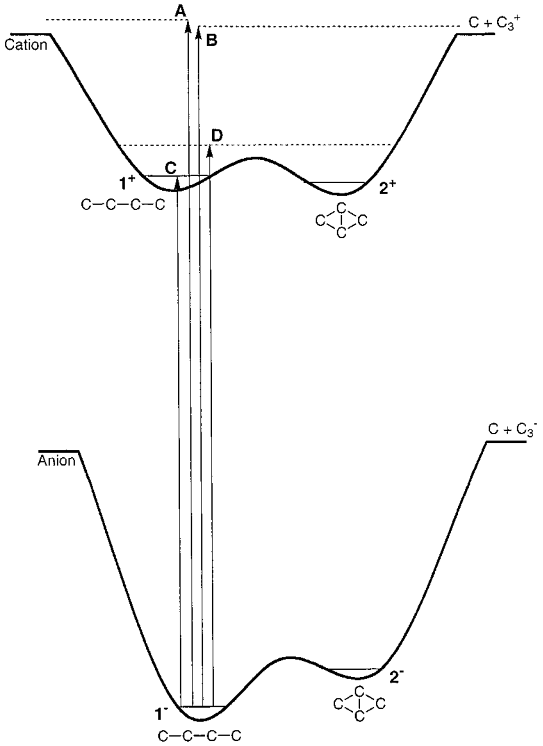

Figure 4. This figure depicts vertical two-electron oxidation of the linear C_4^- anion. Such an oxidation may produce: (A) an excited vibrational state leading to direct dissociation without rearrangement, (B) an excited vibrational state where rearrangement precedes dissociation and thus scrambling of the isotopic label is observed, (C) cold cations, or (D) cations with sufficient energy to rearrange but insufficient energy to decompose. C and D constitute the recovery signal in the $^-$CR$^+$ spectrum (Figure 2a). This schematic is simplified for clarity and shows: (i) only one of the two possible exit channels ($C_4 \rightarrow C + C_3$) and (ii) only a single barrier separating the minima on each surface. See Figures 1 and 3 for a more accurate depiction of each surface.

will be formed with insufficient internal energy to decompose. Such ions form the recovery signal in the $^-$CR$^+$ spectrum (Figure 2a) and while it is not possible to directly establish the structure of these ions, the calculations discussed above suggest that most of these cations will be sufficiently energetic to undergo rearrangement to the rhombic structure. An equilibrium distribution of rhombic and linear structures according to Scheme 3 would be anticipated.

E. Formation of Neutral C_4. The structure and stability of neutral C_4 may be investigated using the anion as a precursor by a neutralization reionization ($^-$NR$^+$) experiment. Here, the incident anion (i) undergoes a one-electron vertical oxidation to the corresponding neutral, (ii) the neutral then has a flight time of 10^{-6} s in which it may rearrange or fragment, and (iii) a second one-electron oxidation generates the corresponding cation, fragmentations of which form the $^-$NR$^+$ spectrum and elucidate the structure of the transient neutral. The $^-$NR$^+$ spectrum of the unlabeled C_4^- anion is given in Table 1 and shows a clear recovery signal at *m*/*z* 48 corresponding to a C_4^+ cation which has been formed by reionization of some stable C_4 neutral. The peak abundances in this spectrum are quite similar to those observed in the $^-$CR$^+$ spectrum, and therefore do not elucidate much about the structure of the final cation or by extrapolation the intermediate neutral. Analysis of the $^-$NR$^+$ spectrum measured for the labeled anion should give some insight into the structure of the intermediate neutral: this spectrum is shown in Figure 2b. While these fragments also occur in the $^-$CR$^+$ spectrum (Figure 2a), the relative abundances differ significantly. Comparison of the losses of ^{13}C and ^{12}C (*m*/*z* 37 and 38, respectively) shows a peak abundance ratio of 5:4 which is approaching the 1:1 ratio indicative of complete scrambling. This represents a significant increase in the randomisation of the label compared to the same ratio in the $^-$CR$^+$ spectrum. Similarly, the abundance distribution of 1.3:6.2:1.0 for the *m*/*z* 24, 25, and 26 ions in the $^-$NR$^+$ spectrum is closer to the statistical 1:4:1 ratio compared to the corresponding ratio in the $^-$CR$^+$ spectrum (see above). Differences in peaks or peak abundances between the $^-$NR$^+$ and $^-$CR$^+$ spectra of a given incident anion, recorded under the same conditions, point to rearrangement of the neutral intermediate.[50,58−60] Part of the scrambling occurring during the $^-$NR$^+$ sequence may be attributed to rearrangement of the reionized C_4^+ cation, as discussed previously. However, the additional randomization noted in this spectrum suggests a similar rearrangement or series of rearrangements occurring for the transient C_4 neutral. Given that previous theoretical studies place neutral rhombic C_4 (**2**) in the same energy regime as the linear species (**1**) the former seems a likely candidate for neutral rearrangement. This possibility is investigated theoretically below.

Table 4. Minima and Transition Structures on the C_4 Neutral Singlet Surface Calculated at the B3LYP/6-31G(d) Level of Theory, with Single Point Energies (including zero-point energy correction) Computed at CCSD(T)/aug-cc-pVDZ

	$C_1{-}C_2{-}C_3{-}C_4$ **^{1}1**	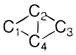 **^{1}2**	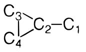 **^{1}3**	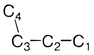 **^{1}TS1/3**	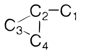 **^{1}TS2/3**
State	$^1\Sigma_g$	^1A_g (^1A_g)^a	$^1A'$	-	$^1A'$
Symmetry	$D_{\infty h}$	C_{2h} (C_{2h})^a	C_S	C_1	C_S
Energy (Hartrees)	-151.65883	-151.67483	-151.63423	-151.61192	-151.63496
Rel. Energy (kcal mol^{-1})	10.0	0.0	25.5	39.5	25.0^b
Bond Lengths (Å)					
C_1-C_2	1.315	1.450 (1.433)^a	1.335	1.330	1.333
C_2-C_3	1.298		1.492	1.349	1.379
C_3-C_4			1.402	1.339	1.429
C_2-C_4		1.497 (1.483)^a	1.419		1.538
Bond Angles (°)					
C_1-C_2-C_3		117.8 (117.6)^a	140.0	183.5	173.4
C_2-C_3-C_4		62.2 (62.4)^a	58.6	89.0	66.4
Dihedral Angles (°)				7.1	

[a] Calculated at the UHF-CCSD/PVTZ level.[10] [b] The zero-point energy corrected single point CCSD(T)/aug-cc-pVDZ energy for the transition structure **TS2/3** places it 0.5 kcal mol^{-1} below **3**. However at the B3LYP/6-31G(d) level, at which these structures were optimized, it is 0.3 kcal mol^{-1} above **3**. We conclude therefore that the barrier to this second cyclization process is negligible, especially as **3**, if formed from **1**, must have at least 14 kcal mol^{-1} excess energy.

F. Rearrangement of C_4. Both singlet and triplet potential-energy surfaces for neutral C_4 have been investigated using the CCSD(T)/aug-cc-pVDZ//B3LYP/6-31G(d) protocol. These calculations predict that linear triplet ($^3\Sigma_g$) and linear singlet ($^1\Sigma_g$) C_4 are separated in energy by only 7.2 kcal mol^{-1} with the triplet being the ground state (Tables 4 and 5). The structural differences between these spin states are negligible (<0.004 Å) which suggests that both have equal probability of being formed from the anion in a vertical (Franck−Condon) oxidation of the type occurring during NR experiments. Consequently, possible rearrangements have been investigated which lead from neutral linear species on both singlet (Table 4) and triplet (Table 5) potential-energy surfaces.

The linear singlet C_4 structure ^{1}**1** is found to be 10 kcal mol^{-1} higher in energy than the rhombus (^{1}**2**) (Figure 5). Rearrangement of linear to rhombic structures is found to be a stepwise process which involves the intermediacy of the C_3-monocyclic

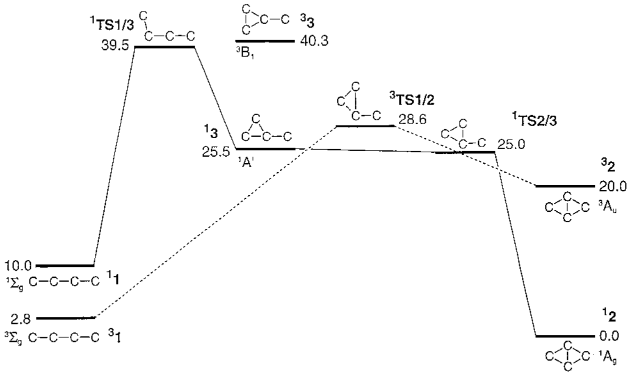

Figure 5. Pathways for the conversion of linear to rhombic C_4 for both singlet (solid line) and triplet (broken line) neutrals. The energies are given in kcal mol^{-1} and were calculated at the CCSD(T)/aug-cc-pVDZ//B3LYP/6-31G(d) level of theory. The geometric details for these minima and transition structures are given in Tables 4 and 5.

Table 5. Minima and Transition Structures on the C_4 Triplet Neutral Surface Calculated at the B3LYP/6-31G(d) Level of Theory, with Single Point Energies (Including Zero-Point Energy Correction) Computed at CCSD(T)/aug-cc-pVDZ.

	$C_1-C_2-C_3-C_4$ **³1**	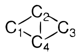 **³2**	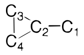 **³3**	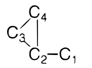 **³TS1/2**
State	$^3\Sigma_g$ ($^3\Sigma_g$)^a	^3A_u	$^3B_1$	$^3A''$
Symmetry	$D_{\infty h}$ ($D_{\infty h}$)^a	C_{2h}	C_{2v}	C_S
Energy (Hartrees)	-151.67039	-151.64241	-151.61054	-151.62918
Rel. Energy (kcal mol^{-1})	2.8^b	20.3	40.3	28.6
Bond Lengths (Å)				
C_1-C_2	1.315 (1.300)^a	1.434	1.322	1.349
C_2-C_3	1.294 (1.278)^a		1.473	1.374
C_3-C_4			1.372	1.353
C_2-C_4		1.578		1.660
Bond Angles (°)				
C_1-C_2-C_3		113.2	152.3	133.5
C_2-C_3-C_4		66.8	62.3	75.0

[a] Calculated at the UHF-CCSD/PVTZ level.[10] [b] Energy in this table is given relative to the lowest energy neutral, namely the singlet rhombic structure **¹2** (Table 4).

minimum **¹3** (Figure 5), which is 15.5 kcal mol^{-1} above **¹1**. Initial cyclization of the linear singlet is reasonably expensive energetically and requires nearly 30 kcal mol^{-1} via the transition structure **¹TS1/3**. Given that (i), the second cyclization step is virtually barrierless through **¹TS2/3**, and (ii) intermediate **¹3** will be formed with 14 kcal mol^{-1} of excess internal energy, the rhombic C_4 neutral should form directly from the linear structure once the initial barrier (**¹TS1/3**) has been surmounted. In fact, the intermediate **¹3** is unlikely to be formed for any significant lifetime in the experiments described here.

The triplet C_4 linear structure (**³1**) may rearrange directly to the more energetic triplet rhombic structure (**³2**) via the transition structure **³TS1/2** (Figure 5): this represents a barrier of 25.8 kcal mol^{-1}. The overall reaction is endothermic by 17.2 kcal mol^{-1}. This is the lowest energy rearrangement pathway on the triplet potential-energy surface: the possible intermediacy of the C_3-monocyclic structure **³3**, is less likely given that it is 37.5 kcal mol^{-1} higher in energy than **³1**. The calculated barriers to isomerization for singlet and triplet fall well below the energies required for the dissociations (i), $C_4 \rightarrow C_3 + C$ and (ii), $C_4 \rightarrow C_2 + C_2$. The endothermicities for these processes have been estimated (from available data[10,76] and based on a linear C_4 structure) to be 122 and 155 kcal mol^{-1} respectively.

A further consideration in this neutral system is the possibility of spin-isomerization. Is it possible for the linear triplet (**³1**) to isomerize to the more stable singlet rhombic structure (**¹2**)? We have not calculated the minimum energy crossing point (MECP) or the spin–orbit coupling for these surfaces, but structural and energetic similarities between C_4 geometries on the singlet and triplet surfaces suggest a low energy MECP of the same magnitude as the barriers already discussed (Figures 3 and 5). Further, there is precedent in the literature for efficient spin crossings among small organic systems.[80–82] Therefore spin-isomerization may provide a further pathway for formation of the stable singlet rhombic structure upon neutralization of the linear anion. The theoretical results presented for neutral C_4 suggest that, on energetic grounds, the rhombic structure is the most probable intermediate in the isotopic scrambling observed in the $^-NR^+$ spectrum. The mechanism for the scrambling via the rhombic structure would be analogous to that proposed for the cation (see Scheme 3).

We now consider the differing degree of isotopic scrambling observed in the $^-CR^+$ and $^-NR^+$ spectra. For the $^-CR^+$ spectrum, the excitations which result in decomposition of the cation without rearrangement (**A**), or with rearrangement (**B**), are shown in Figure 4. For the $^-NR^+$ experiment however, the possible pathways leading to cation fragmentation are more complicated and are illustrated in Figure 6. Upon neutralization of the incident anion a cold linear neutral may be formed with insufficient energy to rearrange (**E**). The Franck–Condon overlap between **1**$^-$ and **³1** is quite good with the minimum excess energy deposited by vertical oxidation of the anion calculated to be only 3.8 kcal mol^{-1}. Similarly, the Franck–Condon overlap between **1**$^-$ and **¹1** provides just 5.7 kcal mol^{-1} excess energy from vertical oxidation. This suggests that many of the neutrals formed in the NR process will have insufficient energy to overcome the barriers to rearrangement. Reionization of the linear neutrals may lead to decomposition with rearrangement (**H**), or without rearrangement (**I**), and concomitant scrambling on the cation surface (cf. $^-CR^+$) with at least 8.3 kcal mol^{-1} deposited by the vertical **³1** → **1**$^+$ transition. Alternatively, neutralization may produce an energetically hot linear neutral with sufficient internal energy to surmount the barriers to isomerization (**F**) producing an equilibrium between linear and rhombic C_4 and scrambling the isotopic label (cf. Scheme 3). Some of these neutrals will decompose upon reionization (**G**) to yield fragments with a statistical distribution of ^{12}C and ^{13}C. The increase in isotopic scrambling between the $^-CR^+$ and $^-NR^+$ spectra is most likely to be due to the intermediacy of neutral rhombic C_4. Such a result might also have been attributed to Franck–Condon effects which may cause different internal energy contents in the ions formed upon $^-CR^+$ and $^-NR^+$. However, for the linear tetracarbon isomers, the Franck–Condon overlaps between (i) anion and neutral and (ii) neutral and cation structures are substantially better than that between the anion and cation structures (see Tables 2–5 and preceding discussion). Therefore, Franck–Condon effects alone would result in a decrease in isotopic scrambling between the $^-CR^+$ and $^-NR^+$ spectra: this is contrary to the experimental results.

---

(78) $\Delta H_f°[(CH_3)_3SiC{\equiv}CC{\equiv}CSi(CH_3)_3]$ is estimated from $\Delta H_f°[H_3SiC{\equiv}CH]$ = 58.1 kcal mol^{-1} [79] and $\Delta H_f°[CH_4]$ = −17.9 kcal mol^{-1},[76] in the following isodesmic reactions: $2\ H_3SiC{\equiv}CH \rightarrow H_3SiC{\equiv}CC{\equiv}CSiH_3 + H_2$ and $H_3SiC{\equiv}CC{\equiv}CSiH_3 + 6\ CH_4 \rightarrow (CH_3)_3SiC{\equiv}CC{\equiv}CSi(CH_3)_3 + 6\ H_2$.

(79) Becerra, R.; Walsh, R. *The Chemistry of Organosilicon Compounds*; Patai, S., Rappoport, Z., Apeloig, Y, Eds.; Wiley: New York, 1998, Vol. 2, Part 1, p 153.

(80) Schröder, D.; Heinemann, C.; Schwarz, H.; Harvey, J. N.; Dua, S.; Blanksby, S. J.; Bowie, J H. *Chem. Eur. J.* **1998**, *4*, 2550.

(81) Aschi, M.; Harvey, J. N. *J. Chem. Soc., Perkin Trans. 2* **1999**, 1059.

(82) Harvey, J. N.; Aschi, M.; Schwarz, H.; Koch, W. *Theor. Chem. Acc.* **1998**, *99*, 95.

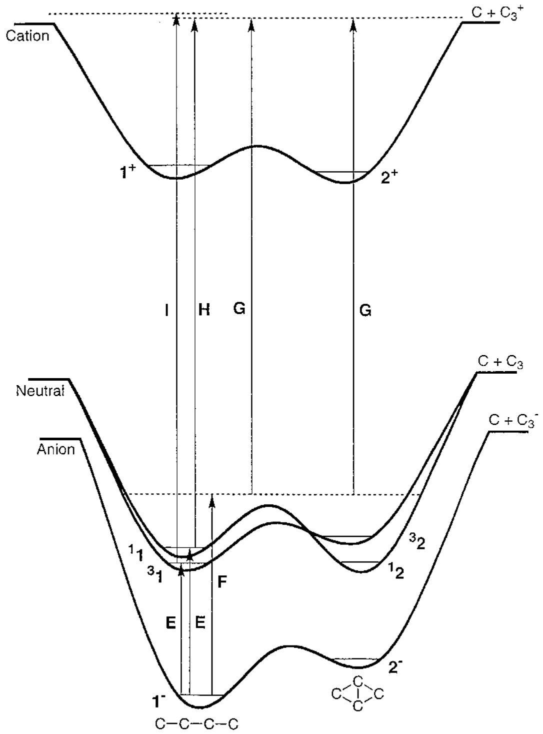

Figure 6. This figure depicts the stepwise vertical oxidations of the linear C_4^- anion. The first oxidation may produce (E), energetically cold linear neutrals on either the triplet or singlet potential surface or (F), internally excited neutrals capable of equilibration between linear and rhombic structures on either the triplet or singlet surface. The latter will lead to scrambling of the isotopic label which will be observed in subsequent dissociative oxidations (G). Some of the energetically cold neutrals (E) which have retained their isotopic distribution will also fragment upon further oxidation. This may occur with (H) or without (I) rearrangement on the cation potential energy surface (cf. Figure 4). This schematic is simplified for clarity and shows (i), only one of the two possible exit channels ($C_4 \rightarrow C + C_3$) and (ii), only a single barrier separating the minima on each surface. See Figures 1, 3, and 5 for a more accurate depiction of each surface.

G. Further Evidence of the Intermediacy of Rhombic C_4. The intermediacy of the neutral rhombus is further supported by $^-NR^-$ experiments carried out on the C_4^- anion and its labeled isotopomer. In each of these experiments the incident anion (i) undergoes vertical one-electron oxidation to the corresponding neutral, (ii) the neutral then has a flight time of 10^{-6} s, when it may rearrange and/or fragment, and (iii) undergo a collisional reduction with xenon gas regenerating the anion. The $^-NR^-$ spectrum of the C_4^- anion (Table 1) features a strong recovery signal, that is, a large peak at *m*/*z* 48 corresponding to the reionized parent. This is indicative of a stable neutral of high electron affinity. However this alone does not identify the structure of the neutral, since both the linear and rhombic forms of C_4 fit these criteria. Similarly, the fragment ions observed in this spectrum corresponding to C_3^- and C_2^- are not characteristic of either structure. The $^-NR^-$ spectrum of the isotopically labeled C_4^- anion is listed in Table 1; this should be compared with the CID spectrum of labeled C_4^- which is also listed in Table 1. As previously discussed, the CID spectrum shows only those fragmentations consistent with terminal ^{13}C labels (eg., $^{13}CC_2^-$ at *m*/*z* 37). The $^-NR^-$ spectrum is much weaker but clearly shows peaks corresponding to losses of ^{13}C and ^{12}C (*m*/*z* 37 and 38) in the approximate ratio 1:1: the error in this ratio is ±20% (over three scans) due to the small abundances of the fragment ions in conjunction with the noise level of the $^-NR^-$ spectrum. The contrast between the CID and $^-NR^-$ spectra of $^{13}CCC^{13}C^-$ is very striking. The CID spectrum demonstrates that rearrangement of the anion does not occur even under collisional activation, while the observation of scrambling in the $^-NR^-$ spectrum can only be accounted for by rearrangement of neutral $^{13}CCC^{13}C$. This may occur by one or more of the pathways investigated in the previous section (see Figure 5), all of which feature the intermediacy of neutral rhombic C_4.

Conclusions

It has been demonstrated that it is possible to generate linear C_4^- in the gas phase by double desilylation of bis(trimethylsilyl)-butadiyne under chemical ionization conditions. CID of the ^{13}C-labeled C_4^- anion confirms a linear structure and suggests that rhombic and/or other isomers are reticent to form even when sufficient energy is supplied. Calculations presented here point to a very small barrier for isomerization of nonlinear C_4^- anions to the more stable linear structure. These experimental and theoretical results seem to fit well with those previous studies of the C_4^- anion where only the linear isomer has been detected:[19,20,23−30] investigations using Coulomb explosion imaging are the exception.[31−33] $^-CR^+$ experiments on the labeled anion demonstrate the propensity of the linear cation to equilibrate with its near isoenergetic rhombic counterpart. This represents the first experimental evidence for the formation of a nonlinear C_4^+ cation in the gas phase, with previous studies having only measured the reactivity of the linear isomer.[35−46] Finally, the $^-NR^+$ and in particular the $^-NR^-$ experiments indicate the intermediacy of a nonlinear neutral C_4. The calculations presented here suggest that on energetic grounds this is the rhombic C_4 structure. This lends support to previous theoretical and experimental studies proposing the stability of this structure in the gas phase.

Acknowledgment. This research was supported by the *Deutsche Forschungsgemeinschaft*, the *Volkswagen-Stiftung*, the *Fonds der Chemischen Industrie*, and the *Australian Research Council*. We thank the South Australian Supercomputing Facility and the Australian National University Supercomputing Facility for generous allocation of computer time. S.J.B. is grateful to the *Deutscher Akademischer Austauschdienst (DAAD)* for financial support.

JA000951C